Appl. Phys. A (2016) 122:400
DOI 10.1007/s00339-016-9849-5

Applied Physics A
Materials Science & Processing

CrossMark

Effect of wavelength and pulse duration on laser micro-welding of monocrystalline silicon and glass

I. H. W. Nordin[1] · Y. Okamoto[1] · A. Okada[1] · H. Jiang[1] · T. Sakagawa[2]

Received: 27 October 2015 / Accepted: 10 November 2015 / Published online: 15 March 2016
© Springer-Verlag Berlin Heidelberg 2016

Abstract Micro-welding characteristics of silicon and glass by pulsed lasers are described. In this study, four types of laser beam, which are nanosecond pulsed laser and picosecond pulsed laser of 532 and 1064 nm in wavelength, were used for joining monocrystalline silicon and glass. Influence of wavelength and pulse duration on micro-welding of monocrystalline silicon and glass was experimentally investigated under the same spot diameter, and the molten area of monocrystalline silicon and glass was characterized. Finally, the breaking strength was evaluated for the overlap weld joint with different pulse duration and wavelength. A splash area of molten silicon around the weld bead line was obvious in the nanosecond pulsed laser. On the other hand, there was no remarkable molten splash around the weld bead line in the picosecond pulsed laser. Breaking strength of specimens with 1064 nm wavelength was higher than with 532 nm wavelength in nanosecond laser, whereas breaking strength of laser-irradiated specimen by picosecond pulse duration was higher than that by nanosecond pulse duration. It is concluded that the combination of picosecond pulse duration and infrared wavelength leads to the stable molten area appearance of the weld bead and higher breaking strength in micro-welding of glass and monocrystalline silicon.

✉ I. H. W. Nordin
ima@ntmlab.mech.okayama-u.ac.jp

[1] Graduate School of Natural Science and Technology, Okayama University, 3-1-1 Tsushimanaka, Kita-ku, Okayama 700-8530, Japan

[2] Kataoka Corporation, 2-14-27 Shinyokohama, Kohoku-ku, Yokohama 222-0033, Japan

1 Introduction

Silicon and glass have been widely used as materials combinations in microelectromechanical systems (MEMS) packaging applications. In many MEMS applications, monocrystalline silicon has been found as the primary substrate material because of its unique electrical, thermal, and mechanical properties. In addition, electrical circuits can be easily fabricated on a monocrystalline silicon surface by a lithography technique as a batch processing, and they can be used as the microelectronic circuitry such as sensor and actuator applications. On the other hand, glass is very popular in MEMS packaging applications due to its excellent mechanical properties, chemically stability, good electrical insulation, and optical transparency, and it has been used to cover electronic microcircuits as a protection in sensor applications [1–4].

In microfabrication technology, many techniques have been adopted as a process of joining monocrystalline silicon and glass. The usage of epoxy to join monocrystalline silicon and glass has been reported [5–7], but its joint properties can be easily changed with environmental humidity and temperature. This point makes it difficult to apply epoxy joining techniques for high-operating temperature applications. In general, the glass with closely matching coefficient of thermal expansion (CTE) to silicon had been chosen as the counterpart material for monocrystalline silicon in anodic bonding. This bonding technique has become the most commonly used technique for joining of silicon and glass in MEMS packaging industries because of its high geometric accuracy and low bonding temperature [8, 9]. However, some limitations such as longer processing time and requirement for wide flat surface have become restrictions of this method. Furthermore, high electrical field produced during the process might lead to a damage of microelectronics.

On the other hand, a micro-joining method such as the use of laser processing method has been proposed to overcome these limitations [10, 11]. Laser micro-welding with its unique characteristic of space selective joining method has the ability of localized heating on materials. Reducing the microstructural damage due to heat and thermal-mechanical stress is useful to perform the minimization of micro-products. Laser processing has not been practically used as the joining method of monocrystalline silicon and glass in MEMS fabrications, but the possibility to implement this micro-joining technique has been successfully reported. Several attempts by utilizing a nanosecond pulsed laser have been done, but the selective laser welding performances of silicon and glass were behind those of anodic bonding [12]. Moreover, recently, an ultrashort pulsed laser with high pulse repetition rate could provide a new technique for a fusion welding of glass and glass [13], and this fusion welding technique can also be applied for joining of glass and silicon. Studies on micro-joining of silicon and glass by using a femtosecond laser pulses have been published [14, 15], and it is reported that filament occurs inside the glass plate corresponding to the high-intensity femtosecond pulsed laser, which led to the lack of energy absorption in the silicon substrate. Picosecond pulsed laser which the laser intensity is below the threshold of multiphoton ionization (MPI) of glass in some optical setups [16], thus permitting more energy to be absorbed at the silicon substrate under slightly weak focusing conditions, was introduced to overcome this problem. It has been reported the welding performance of picosecond pulsed laser particularly on the joint strength was higher than the one in anodic bonding method [17]. However, all these reports on micro-welding of monocrystalline silicon and glass could not clarify the laser–matter interaction sufficiently.

In this study, four types of laser beam which are nanosecond pulsed laser and picosecond pulsed laser with 532 and 1064 nm in wavelength were used for joining monocrystalline silicon and glass. Influence of the processing parameters of wavelength and pulse duration on micro-welding of monocrystallinesilicon and glass was experimentally investigated, and characteristics of the molten area were discussed. Finally, the breaking strength was evaluated by shearing test for the overlap weld joint with different pulse duration and wavelength.

2 Experimental methods

In this study, a laser beam was focused to the interface of silicon and glass from a glass plate side by a f-theta lens of 100 mm in focal length, and laser scanning was carried out by a Galvano scanner to achieve the high-speed laser scanning. The spot diameter was approximately 19 μm. Surfaces of silicon and glass were carefully cleaned to provide optical contact, and both monocrystalline silicon and glass were set in tight contact to avoid clearance. However, it has been assumed that a large optical contact area has an influence on the evaluation of breaking strength. Also, it is reported that the breaking strength increases with increasing the optical contact area [18]. Therefore, a small optical contact area is necessary in order to evaluate the breaking strength of the weld joint precisely. Thus, optical contact area of 1.0 mm in width and 20.0 mm in length was produced by etching monocrystalline silicon with the reactive ion etching (RIE) as shown in Fig. 1a. A laser beam was irradiated on the optical contact area under various processing conditions, and the weld bead was created. Then, the specimen was polished with argon ion beam etching to prepare the cross-sectional surface of the weld bead area as shown in Fig. 1b. The top and sectional surfaces of the weld regions were observed using scanning electron microscope (SEM), and its characteristics were discussed.

Table 1 shows the material properties of the specimens. P-type monocrystalline silicon (100) with 0.675 mm thickness and its counterpart glass material with 1.1 mm thickness of borosilicate glass (Schott, D263) were used as the joint specimens. The shearing test was carried out to measure the breaking load of the overlap weld joints by a Shimadzu EZ-L test machine with a linear guide as shown

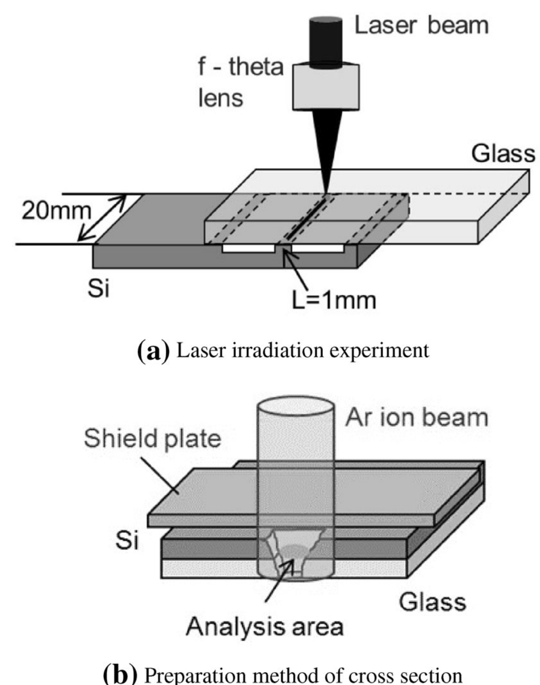

Fig. 1 Schematic diagram of specimen preparation. **a** Laser irradiation experiment. **b** Preparation method of cross section

Table 1 Properties of monocrystalline silicon and borosilicate glass D263

Properties	Silicon	D263
Density ρ [g/cm^3]	2.30	2.51
Specific heat c [J/(kg*K)]	680	820
Melting temp. Θm [K]	1970	1324
Coefficient of thermal expansion $\times 10^{-6}$ [1/K]	3.2	7.2

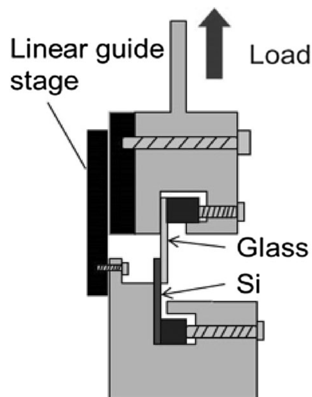

Fig. 2 Schematic illustration of shearing test

in Fig. 2. The linear guide could prevent the specimen from twisting during the shearing test. The specimen was gripped by clampers, which were placed in the fixture blocks. Then, a breaking load was slowly increased until the welded joint of the specimen was fractured. Area of the weld bead was firstly measured, and the breaking strength was calculated by using fracture loads and weld bead areas. This procedure was performed for five times, and the value of breaking strength was the average of five specimens. Finally, the fracture surfaces were observed by SEM. It has been confirmed that the friction force of the linear guide was very small compared with the breaking load.

3 Results and discussion

3.1 Laser irradiation on monocrystalline silicon

The band gap of transparent material such as glass is typically several times higher than the incident photon energy. Therefore, any absorption in the glass plate only occurs, when the intensity is high enough through multiphoton ionization. It is assumed that the laser intensity of picosecond laser is below the threshold of multiphoton ionization of glass under this experimental setup, and therefore, the laser energy was firstly absorbed on the monocrystalline silicon substrate in micro-welding of silicon and glass. For this reason, it is important to have a better understanding of the characteristic of laser-irradiated monocrystalline silicon. In this section, effect of wavelength on the molten area appearance of monocrystalline silicon will be discussed, and the glass plate was not used.

Figure 3 shows the microphotographs of molten area appearance in an individual irradiation spot on monocrystalline silicon for various pulse energies with 532 and 1064 nm wavelength. Nanosecond pulse lasers were used for the comparison of the wavelength. As can be seen from the figure, the molten area became wider with increasing the pulse energy. Moreover, molten splash could be observed at low pulse energy of 5 μJ in the case of 532 nm wavelength, while for 1064-nm wavelength molten splash was observed at high pulse energy of 16 μJ. This phenomenon indicates that temperature increased above the melting point of monocrystalline silicon at low pulse energy in the case of 532 nm wavelength, while 1064 nm wavelength required a high pulse energy. When the laser beam with low pulse energy was focused to the monocrystalline silicon, high absorption rate of 532 nm wavelength resulted in higher energy absorption in monocrystalline silicon compared with that in the case of 1064 nm wavelength.

The absorption coefficients of monocrystalline silicon with 532 nm wavelength and 1064 nm wavelength are $1.0\,\mu m^{-1}$ and $8.0 \times 10^{-2}\ \mu m^{-1}$, which gives optical penetration of 1.0 μm and 400 μm, respectively [19]. Within these dimensions, an illustration diagram of the process was developed as shown in Fig. 4. It can be noticed that the shallow absorption area in the case of 532 nm wavelength indicates that the laser absorption occurred at the area near to the surface, whereas laser absorption area for 1064 nm wavelength was deeper into the bulk material of monocrystalline silicon. These phenomena resulted in a dramatically temperature rise above the melting temperature at the surface of monocrystalline silicon by 532 nm wavelength and gradually increase in temperature for 1064 nm wavelength [20]. Thus, significant amount molten silicon was ejected even at a low pulse energy in the case of 532 nm wavelength because of high absorption rate and shallow absorption area.

3.2 Laser irradiation on monocrystalline silicon and glass

Figure 5 shows microphotographs of molten area appearance at the interface of monocrystalline silicon and glass in an individual irradiation spot observed from the glass plate side. Nanosecond and picosecond pulse lasers with 532 nm wavelength and 1064 nm wavelength were used for the comparison. Laser beams with pulse energies of 9 μJ, 10 μJ and 11 μJ were irradiated to the interface of monocrystalline silicon and glass from the glass plate side. As can be

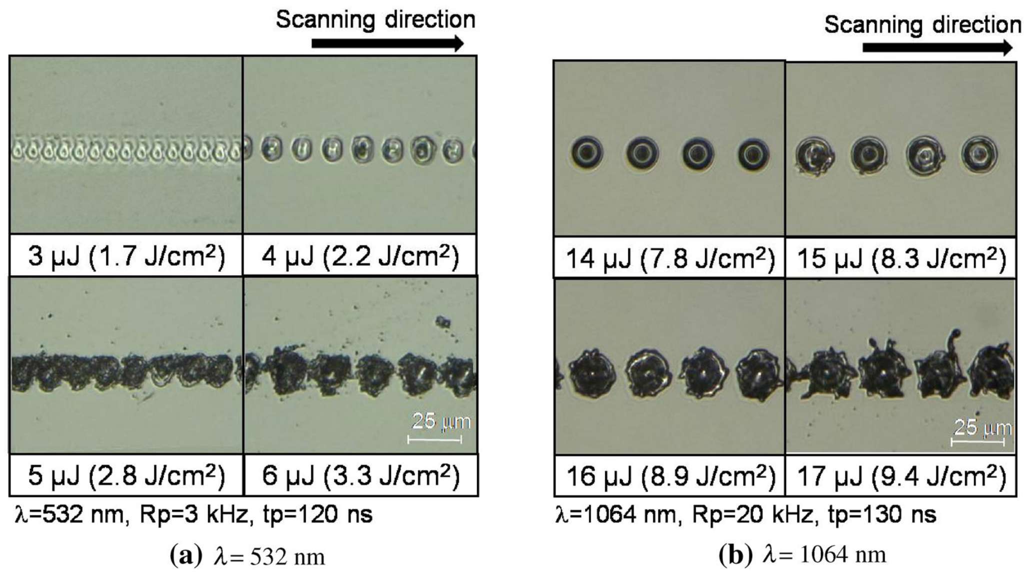

(a) $\lambda = 532$ nm **(b)** $\lambda = 1064$ nm

Fig. 3 Effect of wavelength on molten area appearance of monocrystalline silicon in nanosecond laser

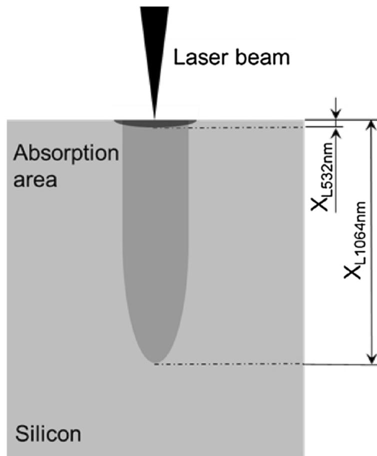

Fig. 4 Schematic illustration on laser absorption of monocrystalline silicon

seen from the figure, molten area increased with the increasing pulse energy. In this first part, effect of wavelength on molten area appearance at the interface of monocrystalline silicon and glass was discussed. A splash area of molten silicon with 532 nm wavelengths was wider than that with 1064 nm wavelength. It is assumed that the shallow absorption area has contributed to increasing size of the molten area. Moreover, molten area appearance was kept stably by 532 nm wavelength even at higher pulse energy of 10 μJ. This case was different from the molten area appearance characteristics by laser irradiation for only on monocrystalline silicon, where molten splash could be observed at lower pulse energy. It is considered that glass plate on the top of silicon substrate has influence on the

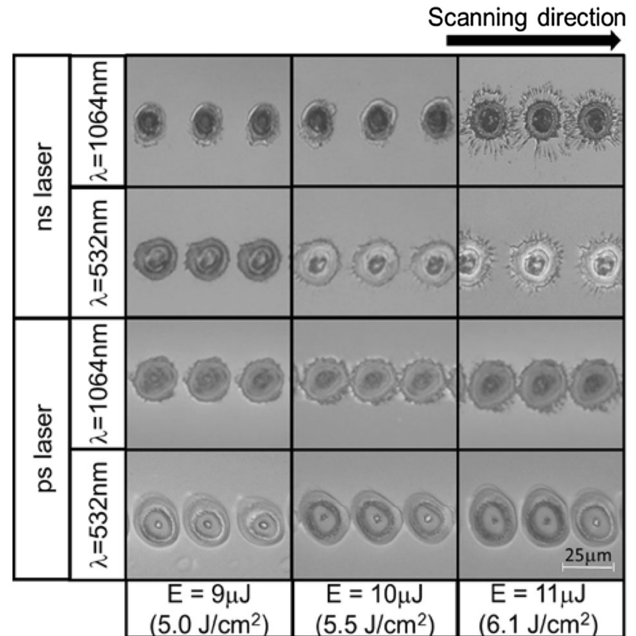

Fig. 5 Effect of pulse duration and wavelength on molten area appearance of monocrystalline silicon and glass

generation of the molten splash. When glass plate was placed to cover silicon substrate with tight contact, compressive force between the joint specimens acts to increase the pressure at the interface of monocrystalline silicon and glass. Hence, the molten area appearance was kept stably even at high pulse energy.

Next, the effect of pulse duration on molten area appearance the interface of monocrystalline silicon and glass is discussed. Stable molten area appearance was

observed in picosecond pulse duration compared with that in nanosecondpulse duration by both 532 nm and 1064 nm wavelength as shown in Fig. 5. In addition, molten area appearance in nanosecond pulse laser changed drastically at pulse energy of 11 µJ. This phenomenon indicates that temperature rose above the melting point of monocrystalline silicon at least. On the other hand, picosecond pulsed laser still kept a stable molten area appearance even at pulse energy of 11 µJ. Therefore, it is considered that the silicon substrate was heated mildly by a picosecond laser.

Figure 6 shows the weld beads created at high overlap rate. It can be observed that molten splash around the weld bead line was obvious in the case of nanosecond laser as shown in the figure. On the other end, no remarkable molten splash was found around the weld bead line in the case of picosecond laser, which indicates that the substrate was heated mildly. It is considered that shorter pulse length of picosecond pulse duration resulted in higher power densities, which led to rapid heating and earlier evaporation of the monocrystalline silicon compared with that in nanosecond pulse laser. This explains the amount of the molten splash reduced after the irradiation by picosecond laser.

Figure 7 shows the backscattered electron images of the cross section around the interface between silicon and glass for laser irradiation condition of pulse energy 3µJ, pulse repetition rate 300 kHz and scanning velocity 0.5 m/s. X-ray element mappings of oxygen and silicon were also performed on the same area. The elemental analyses were performed to identify the element distribution at the joint area by using a energy-dispersive spectroscopy. Laser beam with 532 and 1064 nm wavelength of picosecond laser was used in order to discuss the effect of wavelength on the micro-welding of silicon and glass. Although the coefficient of thermal expansion (CTE) of D263 glass is higher than that of monocrystalline silicon, a crack-free micro-welding of silicon and glass was obtained by picosecond pulsed laser. In the case of laser-irradiated specimen by 1064 nm wavelength, a little diffusion of silicon material into glass part can be observed, where the interface shows a flow pattern that curved toward the laser axis into the glass part. This suggests that high temperature was achieved near the area of the curved structured. It is considered that silicon substrate firstly absorbed the laser energy, since the laser intensity was below the threshold of MPI of glass. The absorption of laser energy caused the melting of the silicon material. Then, the glass was indirectly heated by the heat convection from the molten silicon and heat conduction from the silicon substrate. The changing state of the glass material leads to the direct absorption of the laser energy in the glass part. This process provides temperature rise of the glass material at least above its forming temperature. On the other hand, in the case of laser-irradiated specimen by 532 nm wavelength, the joint structure was almost visible as a flat structure. Here, it is believed that most of the laser energy was absorbed in the silicon material due to high absorptivity of 532 nm wavelength, which resulted in insufficient energy to heat up the glass substrate.

Furthermore, hole structure is observed at the interface of the joint area for both laser wavelengths, when the pulse energy is increased to 4 µJ and 5 µJ as shown in Fig. 8. These hole structures are not desirable in micro-welding of silicon and glass, since it might reduce the strength of the joint due to the existence of vacancies. However, characteristics of laser absorption for different wavelength on the formation of the hole structure can be distinguished. It

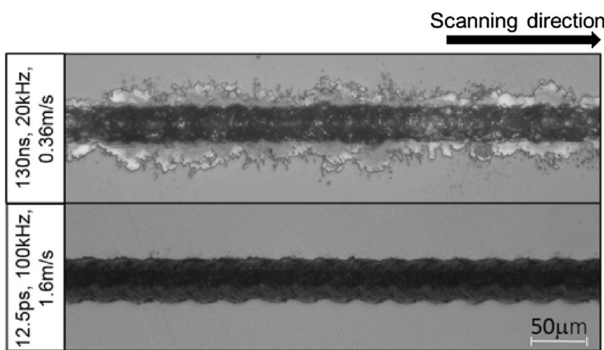

Fig. 6 Weld bead created at high overlap rate ($\lambda = 1064$ nm, $E = 11$ µJ (6.1 J/cm^2), overlap rate 90 %)

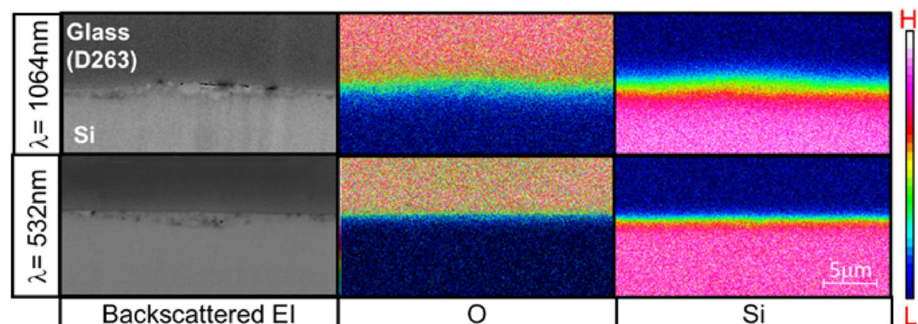

Fig. 7 Element analysis at the interface of glass and monocrystalline silicon ($E = 3$ µJ, $R_p = 300$ kHz, $v = 0.5$ m/s, $t_p = 12.5$ ps, overlap rate 90 %)

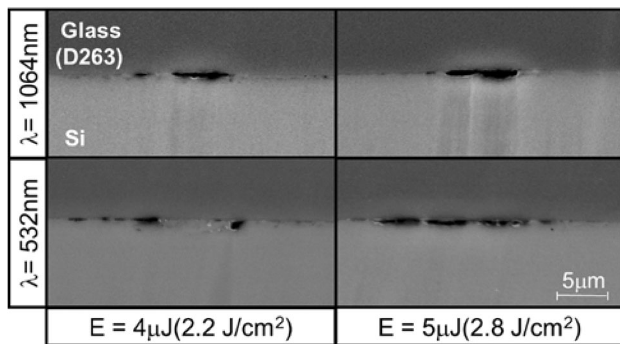

Fig. 8 SEM images at the interface of monocrystalline silicon and glass (R_p = 300 kHz, v = 0.5 m/s, t_p = 12.5 ps, overlap rate 90 %)

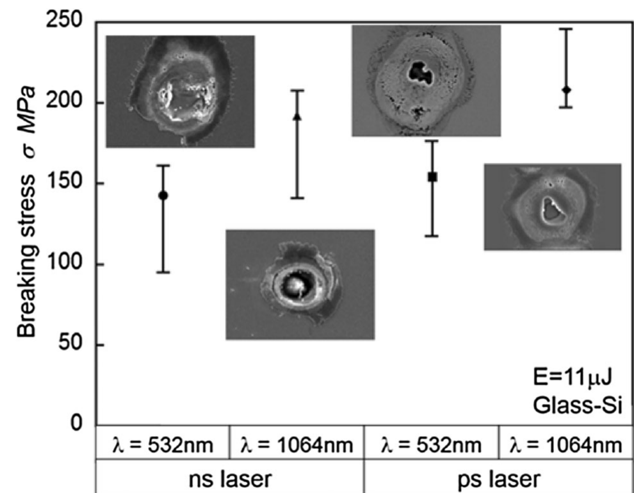

Fig. 9 Breaking stress of monocrystalline silicon and glass joint

could be observed that the hole structure was wider in 532 nm wavelength compared with that in 1064 nm wavelength. Wide hole structure, and elongate horizontally indicates shallow absorption areas in 532 nm wavelength, whereas narrow hole structure indicates deep absorption areas in 1064 nm wavelength.

In micro-joining process, it is well agreed that joint strength is increased, when diffusion of joint material was occurred. Therefore, selection of 1064 nm wavelength in micro-welding of silicon and glass is becoming priority. Moreover, it has been reported the formation of anchor geometry at the joint interface of silicon and glass under high pulse repetition rate of picosecond laser with 1064 nm wavelength. The structure was more likely a tangled structure, where both silicon and glass were mixing and twisting together to appear an "anchor" as a result of the laser irradiation. It is also reported that the breaking strength is increased corresponding to the anchor effect of the tangle structure [17].

3.3 Evaluation of the breaking strength

Figure 9 shows shearing test results on micro-joining of monocrystalline silicon and glass in an individual irradiation spot. Nanosecond and picosecond pulse lasers with 532 nm wavelength and 1064 nm wavelength were used for the comparison. Laser pulse energy was kept constant at 11 μJ. Fracture surfaces of the weld specimen after the shearing test were observed by SEM. For effect of wavelength, breaking strength for laser-irradiated joint specimen with 1064 nm wavelength was higher than that with 532 nm wavelength as shown in the figure. It is well explained as the fracture surface of the weld specimen confirmed that molten area for laser-irradiated specimen with 532 nm wavelength was wider than that with 1064 wavelength, which has a significant effect on the joint strength.

Furthermore, for effect of pulse duration, breaking strength for laser-irradiated joint specimen with a picosecond laser shows higher value than that with nanosecond laser. Fracture surface for laser-irradiated specimen with picosecond pulse duration appeared to be a flat surface. On the other hand, molten splash area could be noticed on the fracture surface of laser irradiation condition with nanosecond pulse duration which gives clear evidence for lack of breaking strength of the weld specimen. Molten splash might generated the gap between the interfaces of joint material.

In this study, higher breaking strength could be obtained by the combination of picosecond pulse duration and near-infrared wavelength. As a conclusion, proper selection of processing parameters was necessary to obtain good-quality joining of monocrystalline silicon and glass. In addition, advantages of the technique such as no need for pre- and post-heating, high joining rate and capability for space selective welding have made it unique for future development of high efficiency and reliable micro-joining technique of silicon and glass.

4 Conclusions

Micro-welding of monocrystalline silicon and glass was experimentally investigated, and effects of the wavelength and pulse duration were clarified. The main conclusions obtained in this study are as follows:

1. Area of molten splash with 532 nm wavelength was wider than that with 1064 nm in a nanosecond pulsed laser.
2. Molten splash appeared suddenly at more than a boundary pulse energy in nanosecond pulsed laser. On

the other hand, picosecond pulse laser still kept a stable molten area appearance even at the same boundary pulse energy, and a stable molten behavior could be obtained even at high overlap rate condition.

3. The combination of picosecond and infrared wavelength showed stable molten area appearance in the micro-welding of glass and monocrystalline silicon.
4. The joint interface between silicon and glass revealed the diffusion of silicon material into glass parts in 1064 nm wavelength, while almost flat surface in 532 nm wavelength.
5. Breaking strength of specimen with 1064 nm wavelength was higher than that with 532 nm wavelength. On the other hand, breaking strength of laser-irradiated specimen by picosecond pulse duration was higher than that by nanosecond pulse duration.

Acknowledgments The authors would like to thank Prof. Dr. Isamu Miyamoto (Osaka University) and Prof. Dr. Yoshiyuki Uno (Chugoku Polytechnic College) for helpful discussion during writing this manuscript. This work was partially supported by Japan Society of the Promotion Science (JSPS) KAKENHI Grant No. 24760107.

References

1. A.G. Darrin, R. Osiander, in *MEMS Packaging Materials*, ed. by R. Ghodssi, P. Lin (Springer, Boston, 2011)
2. S.A. Audep, M.E. Katrina, *International conference on Solid-state Sensors and Actuators* (Chicago, 1997), pp. 287–289
3. J. Baborowski, A. Pezous, D.G. Spinola, R. Jose James, R. Ziltener, C. Muller, M.A. Dubois, Proced. Chem. **1**(1), 153538 (2009)
4. M. Chiao, Y.T. Cheng, L. Lin, in *Introduction to MEMS Packaging*, ed. by Z. Zhou, Z. Wang, L. Lin (Springer, Berlin, 2012), pp. 415–446
5. R.L. Smith, S.D. Collins, IEEE Trans. on Electron Devices **35**, 787–792 (1988)
6. A.S. Laskar, B. Blythe, Sens. Act. A **36**, 1–27 (1993)
7. R. Joyce, K. Singh, H. Sharma, S. Varghese, J. Akhtar, J. Microsyst, Technol. **20**(6), 1153–1158 (2013)
8. J. Wei, H. Xie, M.L. Nai, C.K. Wong, L.C. Lee, J. Micromech. Microeng. **13**, 217–222 (2003)
9. A. Cozma, B. Puers, J. Micromech. Microeng. **5**, 98–102 (1995)
10. N. Lorenz, M.D. Smith, D.P. Hand, J. Microelectron. Reliab **51**, 2257–2262 (2011)
11. Y.T. Cheng, L. Lin, K. Najafi, J. Microelectromech. Syst. **9**, 3–8 (2000)
12. U.M. Mescheder, M. Alavi, K. Hiltmann, C. Lietzau, C. Nachtigall, H. Sandmaier, Sens. Act. **97–98**, 422–427 (2002)
13. M.J. Wild, A. Gillner, R. Poprawe, Sens. Act. A **93**, 63–69 (2001)
14. T. Tamaki, W. Watanabe, K. Itoh, Opt. Express **14**, 10460–10468 (2006)
15. A. Horn, I. Mingareev, A. Werth, M. Kachel, U. Brenk, Appl. Phys. A **93**, 171–175 (2008)
16. I. Miyamoto, K. Cvecek, Y. Okamoto, M. Schmidt, H. Helvajian, Opt. Express **19**, 22961–22973 (2011)
17. I. Miyamoto, K. Cvecek, Y. Okamoto, M. Schmidt, Appl. Phys. A **114**, 1–22 (2014)
18. Y. Okamoto, I. Miyamoto, K. Cvecek, A. Okada, K. Takahashi, M. Schmidt, J. Laser Micro/Nanoeng. **8**, 65–69 (2013)
19. K. Stolberg, B. Kremser, S. Friedel, Y. Atsuta, J. Laser Micro/Nanoeng. **4**, 231–233 (2009)
20. Q. Lu, S.S. Mao, X. Mao, R.E. Russo, J. Appl. Phys. **104**, 083301–083307 (2008)